

Voltage Generation in Piezoelectric Energy Harvesting with Magnet: FEA Simulation and Experimental Analysis

Muhammad Imran Jaafar¹, Hossameldin M.M.M. Rabah¹, N.H. Diyana Nordin^{1*}, Asan G.A. Muthalif², Azni N. Wahid¹

¹Smart Structures, Systems and Control Research Lab (S³CRL), Kulliyah of Engineering, International Islamic University Malaysia, Kuala Lumpur, 53100 MALAYSIA

²Department of Mechanical and Industrial Engineering, College of Engineering, Qatar University, Doha, QATAR

*Corresponding Author

DOI: <https://doi.org/10.30880/jst.2021.13.02.003>

Received 21 April 2021; Accepted 19 Oktober 2021; Available online 2 December 2021

Abstract: Energy harvesting devices are needed as an alternative to batteries as it is costly to power up wireless sensor network. However, the power generated and operating bandwidth for the typical energy harvester are still compromised. Therefore, in this work, the use of permanent magnet in Piezoelectric Energy Harvester (PEH) is proposed to increase the operating bandwidth. A simulation study was conducted using COMSOL Multiphysics software to observe the effect of mechanical tuning using magnet on the voltage produced. It shows that PEH with oscillating magnetic field is capable of reaching generated peak power of 0.775 mW and increase the operating bandwidth by 10%. Experimental setup was also fabricated to further validate the observation at different polarities and varying distances with permanent magnets. It is observed that while the peak power achieved in the attractive mode is smaller as compared to its counterpart, however, its bandwidth is larger.

Keywords: piezoelectric energy harvesting, COMSOL, operating bandwidth, PEH with magnet, frequency tuning

1. Introduction

As technology continues to advance, current trends show that most devices and research have evolved towards small and low-power electronics. The dependency of these devices to battery as the main power source is inclining to the fact that battery has limited lifespan and is not cost effective for long term deployment. Therefore, in order to provide power sources for self-sustainable electronic devices, the concept of energy harvesting system is introduced in these applications. This option offers the solution to overcome the limitation of battery-based devices and has become popular recently especially in the wireless sensor network application.

There are a number of ambient energies that can be harvested and collected for the use of energy conversion to electrical energy such as solar [1], vibration [2]–[4] and electromagnetic waves [5], [6]. However, harvesting energy from vibrations is of interest as it is more ubiquitous compared to other ambient energy sources. In vibration energy harvesting, there are three methods of producing electricity which are by the means of electrostatic, electromagnetic and piezoelectric [7]. Nevertheless, the focus of this paper is on the piezoelectric technique. Piezoelectric material is a smart material capable of producing electricity when subjected to mechanical stress [7], [8].

Early designs of piezoelectric energy harvester utilise the use of rectangular cantilever beam to generate the voltage, namely unimorph [9], [10] and bimorph [11] piezoelectric energy harvester. As the names suggest, unimorph setup requires one film of piezo attached on top of the cantilever beam, while bimorph setup involves two films

attached on the top and bottom layers of the beam. Bimorph setup proved to be more advantages than that of unimorph [12], [13].

The geometry of the piezoelectric cantilever beam incredibly influences its vibration collecting capacity as well. Truncated shape such as triangular [4], [14], [15] and trapezoidal with rectangular cross segments proven to be better energy harvester as compared to the traditional design due to a more uniform strain distribution along the beam. To use this type of energy harvester, the resonance of the surrounding needs first to be assessed as the properties of the whole structure is fixed, thus resulting to a fixed natural frequency and frequency bandwidth.

Complex shape such as spiral-shaped piezoelectric energy harvester [16], [17] and L-shaped structure [18] managed to increase the number of resonant frequencies. However, these designs might be complicated and incur higher cost to be fabricated. Though, a number of researchers do also venture into concave [19], [20] and convex [21] shaped piezoelectric energy harvester, nevertheless, these designs require limited choices of piezoelectric material due to its flexibility requirement. Consequently, these designs are often seen in wearable devices. In addition, an array of cantilever beams can also be used as one of the multi modal energy harvester techniques [22], [23]. This is due to the fact that each beam has its own natural frequency. Therefore, more power and a wider frequency bandwidth can be harvested. However, using multi-modal energy harvester might not be appropriate in micro scale devices as it tends to be larger in size.

As mentioned before, ambient energy in the form of vibration is usually low in amplitude and frequencies. Several system designs and techniques have been proposed by the researchers, to overcome the limitations of the narrow bandwidth, high natural frequencies and low output power. In general, the linear energy harvesting is preferred amongst other techniques, as no external source of energy to tune the system is required. Moreover, the design is simple and easy. However, for the resonance tuning method, it needs to be adjusted manually. They are characterised by a very narrow frequency bandwidth near to the resonance and have an optimum performance within the resonance frequency only. Therefore, it requires a certain excitation frequency to reach the optimum performance. If there is a slight change in the excitation frequency, the system performance decreases rapidly due to the narrow bandwidth. Accordingly, developing an energy harvester with a wide frequency bandwidth spectrum becomes one of the major concerns and interests for many researchers.

In this work, a non-linear energy harvesting technique, through the use of fixed magnets on a piezoelectric energy harvester beam is discussed. This paper consists of 4 sections. Section 1 discusses the background and motivation for this study. On the other hand, Section 2 presents the simulation study of piezoelectric energy harvester using COMSOL Multiphysics software and Section 3 discusses the experimental work related to the title. Section 4 concludes the work.

2. Simulation Studies of Piezoelectric Energy Harvester using COMSOL Multiphysics Software

In this paper, in order to study the effect of adding magnetic field to the conventional piezoelectric energy harvester configuration, a simulation study was first conducted using COMSOL Multiphysics software. This software was chosen as there were limited resources that includes the effect of magnetic field on the performance of piezoelectric energy harvester using COMSOL Multiphysics software. Several parameters of the piezoelectric energy harvester model were given fixed values for ease of computation, as listed in Table 1.

Table 1 - List of parameters assigned to the PEH

Description	Value
Magnetic dipoles 1, m_1	0.019 Am ²
Magnetic dipoles 2, m_2	-0.019 Am ²
Initial distance between m_1 and m_2	0.015 m
Beam dimension ($w \times l \times t$)	5.00 × 21.00 × 0.16 mm
Permanent magnet dimension ($w \times l \times t$)	5.00 × 4.00 × 1.70 mm
Fixed end block dimension ($w \times l \times t$)	1.00 × 1.00 × 5.00 mm

The magnetic dipoles are set to be in attractive modes, which are indicated by the negative sign of m_2 and m_1 's positive sign represents repulsive mode. The values are taken from study by Tang and Yang (2012). The PEH is modelled as a bimorph piezoelectric beam structure, equipped with a magnetic block as the proof mass at the free end of the beam and copper beam as the substrate (as shown in Fig. 1). The dimensions of the beams are identical, which are at 21 × 0.16 × 5 mm. The fixed end of the beam is attached to a solid structure to produce base excitation. Two permanent magnets were used, one being embedded inside the proof mass, and another magnet is assumed to face the proof mass at its widest cross-sectional area.

Four materials were chosen to be the elements of the piezoelectric energy harvester which are Lead Zirconate Titanate (PZT-5H), structural steel, copper and neodymium. Fig.1 shows the materials in their assigned domain of the structure.

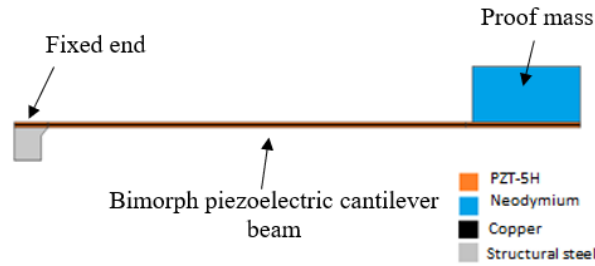


Fig. 1 - Type of materials used in COMSOL multiphysics software

2.1 Boundary Condition

The simulation was done in ‘*solid mechanics*’ physics. The whole cantilever acts as linear elastic materials with damping except for PZT-5H. It is assumed that the whole system has zero initial displacement and structural velocity. The boundaries of the whole structure were set to be free excluding the base of the support structure which was assigned as ‘*fixed constraint*’. The excitation force of the Piezoelectrical Energy Harvester was introduced as ‘*Body Load*’ and can be expressed as in Eq. (1).

$$F_{ex} = \rho_s \times g \times acc \quad (1)$$

where ρ_s , g and acc are density, gravitational constant and base acceleration, respectively. The gravitational constant was set at 1 g throughout the simulation.

The presence of the magnetic force as a boundary load acting on the proof mass can be written as:

$$F_{mag} = -\frac{3\tau m_1 m_2}{2\pi(u_1(t) - u_2(t) + D_0)^4} \quad (2)$$

where m_1 and m_2 are the moments of magnetic dipoles for magnet 1 and 2, τ is the vacuum permeability and D_0 the initial distance between the two magnetic dipoles [24]. The displacement of both magnetic proof mass and magnetic oscillator needs to be considered and they are denoted as $u_1(t)$ and $u_2(t)$ distinctively. However, since only fixed magnet is of interest in this study, therefore, $u_2(t)$ is not considered.

The piezoelectric layers are also subjected to ‘*zero electric potential*’ so that the voltage produced can be measured across it. The boundaries that are exposed to the free space or air is considered as ‘*terminal*’ while the boundaries that is in contact with the copper beam is the ‘*ground*’. The setting of the meshing was set to be tetrahedral with normal element size to reduce the computation time as finer material requires more computation. This step is essential for the process of simulation as precaution against undistributed load along the structure and irregular or faulty results.

2.2 Results

2.2.1 Mode Shape

The deformation of the beam at the first natural frequency is shown in Fig. 2 at around 71 Hz. Its associated stress analysis of the mechanical system, as depicted in Fig. 3 shows that the stresses is highly concentrated at the clamped area of the cantilever beam throughout the simulation. This result also indicates that for a rectangular cantilever beam, a higher voltage will be generated at the fixed end.

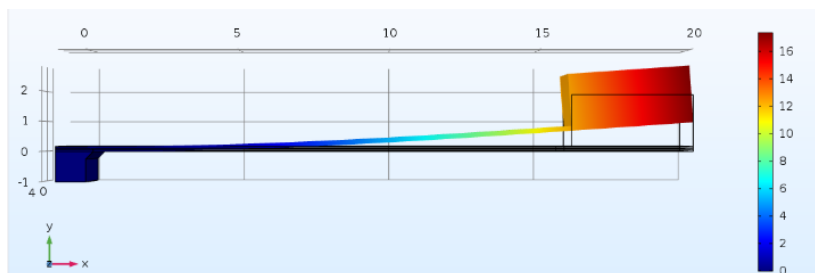


Fig. 2 - The first mode shape of the system

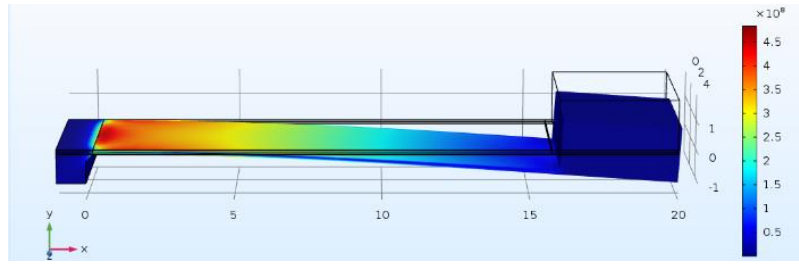


Fig. 3 - Stress distribution on the piezoelectric cantilever beam

2.2.2 Power and Voltage Generation

The performance of the PEH with magnetic oscillator shows a promising result, as observed in Fig. 4. The voltage generation in the system does increase by 80 mV in magnitude compared to the conventional PEH. In Fig. 4(c), in the case of magnetic oscillator, it is seen that the resonance frequency of the beam shifted to the right with the presence of the magnetic force.

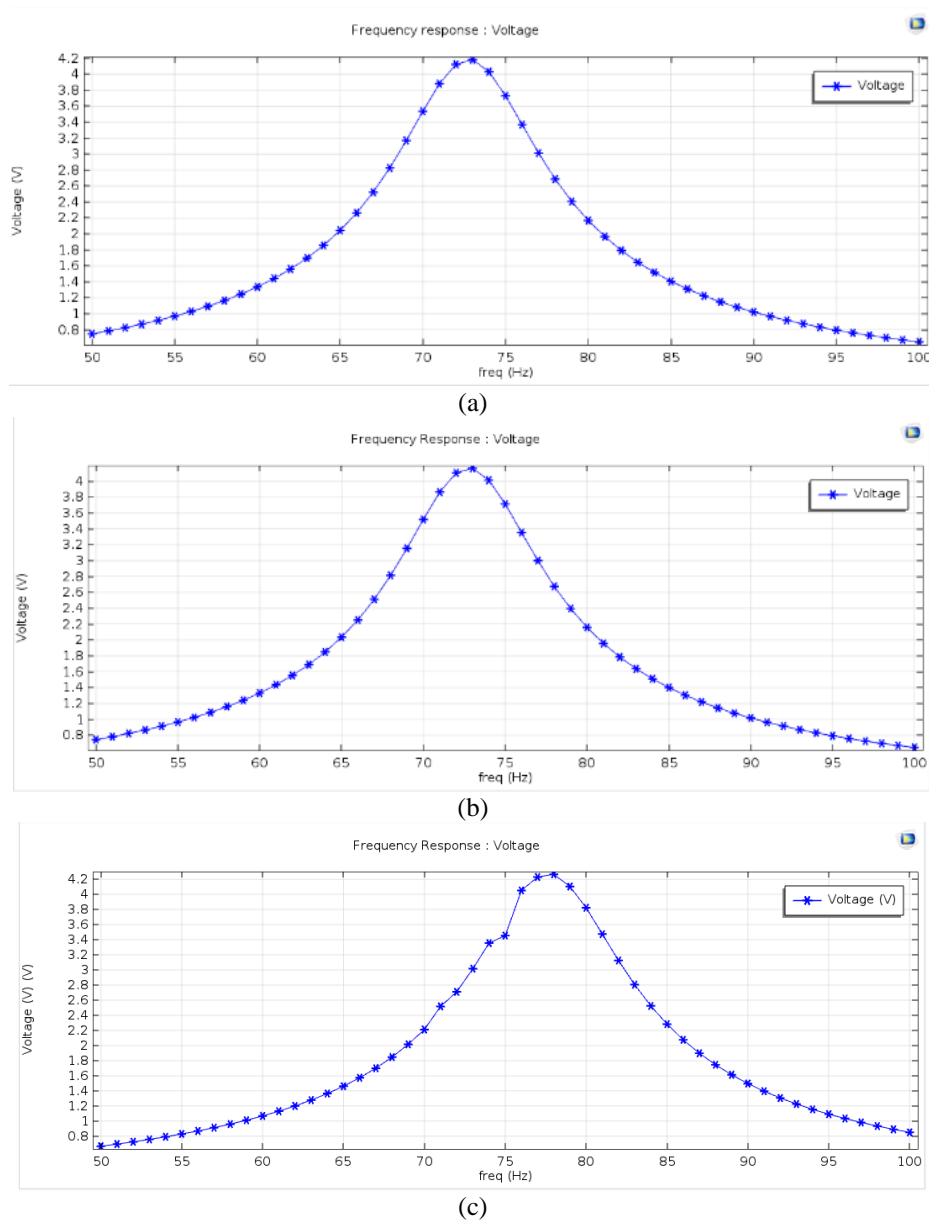


Fig. 4 - Voltage generation of a) conventional PEH; b) PEH with fixed magnet; c) PEH with magnetic oscillator

For the PEH with fixed magnet, the pattern of the voltage generation graph is almost identical with the conventional PEH. The difference is hard to notice from the graph as it is only 20 mV in magnitude. The addition of fixed magnet to conventional PEH does not improve the performance and even decrease the voltage generation of the PEH. Both systems achieved their highest amplitude of voltage generation at 73 Hz.

The performance of the PEH with magnetic oscillator shows a promising result. The voltage generation in the system does increase by 80 mV in magnitude as compared to the conventional PEH. However, it is seen that the natural frequencies shifted to the right, indicating an increase in natural frequency. In the case of the PEH with magnetic oscillator, the performance of the system is more developed with the presence of the magnet. When both PEH and magnetic oscillator oscillate simultaneously, they are also transferring the vibration energy of their individual system through magnetic interaction to each other.

One of the factors that contribute to the very small changes in the results of Fig. 4(a) and Fig. 4(b) might be due to the distance between the magnets as the tip mass, to the other source of magnetic field. In Fig. 4(c), the effect is more significant as the magnetic interaction is larger as it oscillates. Hence, the increase of frequency bandwidth is more visible.

Simulation results of the PEH with fixed magnet, as shown in Fig. 5 shows small discrepancy from the conventional PEH. The fixed magnet model falls short of electric power output than its standard model. The power output stood at 0.721 mW when the system is at its natural frequency. PEH with magnetic oscillator model generates around 0.75 mW which surpassed the standard model. An increase of 10% of operating bandwidth is shown on the simulation as the purposed model has a bandwidth of 24 Hz while the standard model only has 22 Hz bandwidth.

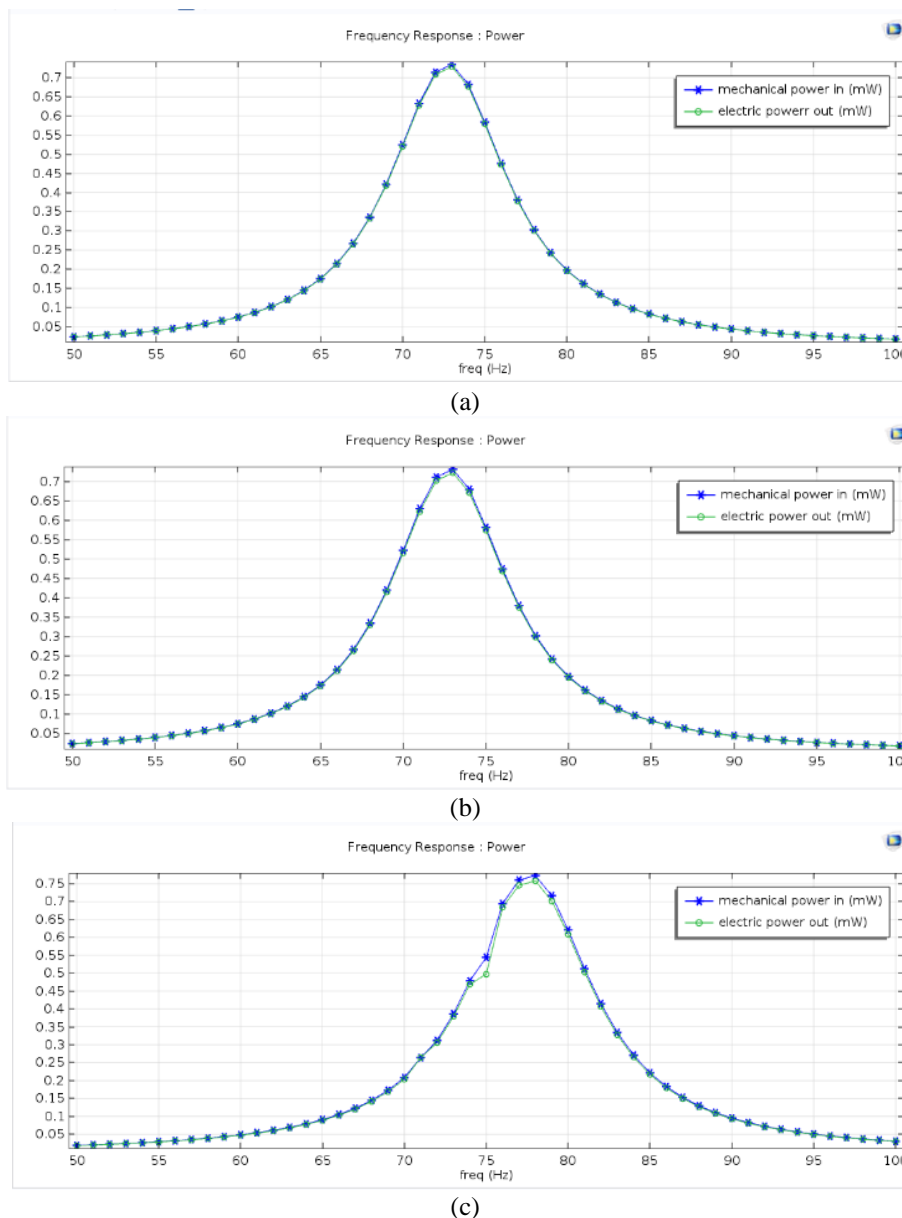


Fig. 5 - Comparison of power in and power out of a) conventional PEH; b) PEH with fixed magnet; and c) PEH with magnetic oscillator

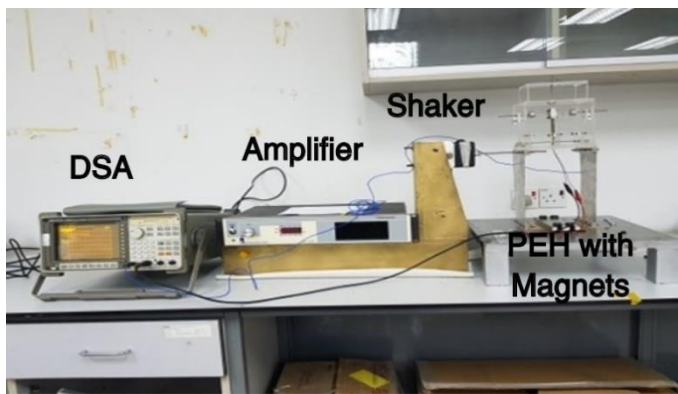
The explanation for the changes in performance of both PEH with fixed magnet and PEH with magnetic oscillator is the magnetic interaction of the system. In the fixed magnet model, the magnetic interaction act as resistor to the strain of the PEH as it does not vibrate. It induces more stiffness to the structure. The increase performance in magnetic oscillator model is due the fact that the dynamic of the magnet contributes to the vibration of the system. Overall, from the simulation studies, it shows that the use of magnetic force in a PEH system does increase the bandwidth frequency.

3. Experimental Setup of Piezoelectric Energy Harvester

Experimental validation was also conducted to study the effect of the presence of magnetic field at two different magnet polarities, as well as varying the distance between the two magnets. In this experiment, measurements were taken at both attractive and repulsive modes at three different distances which are 1.5 cm, 2 cm and 3 cm, respectively. In this work, only the case of fixed magnet was considered. The parameters used in the experiment is listed in Table 2 and the arrangement of the experimental setup is shown in Fig. 6. The placement of the magnet, with respect to the piezoelectric can be clearly seen in Fig. 6(b).

Table 1 - System parameters used in the experiment

Description	Symbols	Value	Units
The beam composite and tip mass			
Composite beam dimension ($w \times l \times t$)		$25.40 \times 71.00 \times 0.71$	mm^3
Young modulus of copper	E_c	110×10^9	N/m^2
Young modulus of FR4	E_f	26×10^9	N/m^2
Magnetic tip mass of PEH	M_t	27.50	g
Distributed mass of beam	M_b	3.12	g
Piezoelectric element			
Piezoelectric material dimension ($w \times l \times t$)		$20.80 \times 46.00 \times 0.18$	mm^3
Young modulus of piezoelectric patch	E_p	63×10^9	N/m^2
Clamp capacitance	C^s	97×10^{-9}	F
Loss Factor	η	0.02	-
Fixed magnets			
Length of magnet	l_m	2.75	mm
Diameter of magnet	d_m	12.00	mm
Surface flux (magnetic flux density)	β	-	Tesla
Permeability of medium	τ_0	$4\pi \times 10^{-7}$	H.m^{-1}



(a)



(b)

Fig. 6 - (a) Experimental setup; (b) PEH with one fixed magnet configuration

The experimental results for the PEH with one of side magnets are shown in Fig. 7. The presence of magnet managed to tune the natural frequency of the system. Here, the PEH without magnet is taken as the benchmark. It is obvious that the resonance frequency of the PEH increases when the magnets are repulsive, as is shifted to only 12.82 Hz at 1.5 cm from the beam from 11.59 Hz (the benchmark frequency). However, it has a considerable decrement while they are in attractive mode whereas it is shifted to 8.3 Hz at 1.5 cm away from the PEH from the benchmark frequency. The variations of the resonance frequency are due to the existence of the magnetic field. In the attractive mode, there is an additional force applied to the beam that eases the bending, therefore, it leads to lower natural frequencies. However, in repulsive mode, the magnets are moving away from each other that leads to additional stiffness for the beam and make it harder to bend, hence, increases the natural frequency. The bandwidth is almost consistent for all given distances at the repulsive mode as well as the peak output voltage.

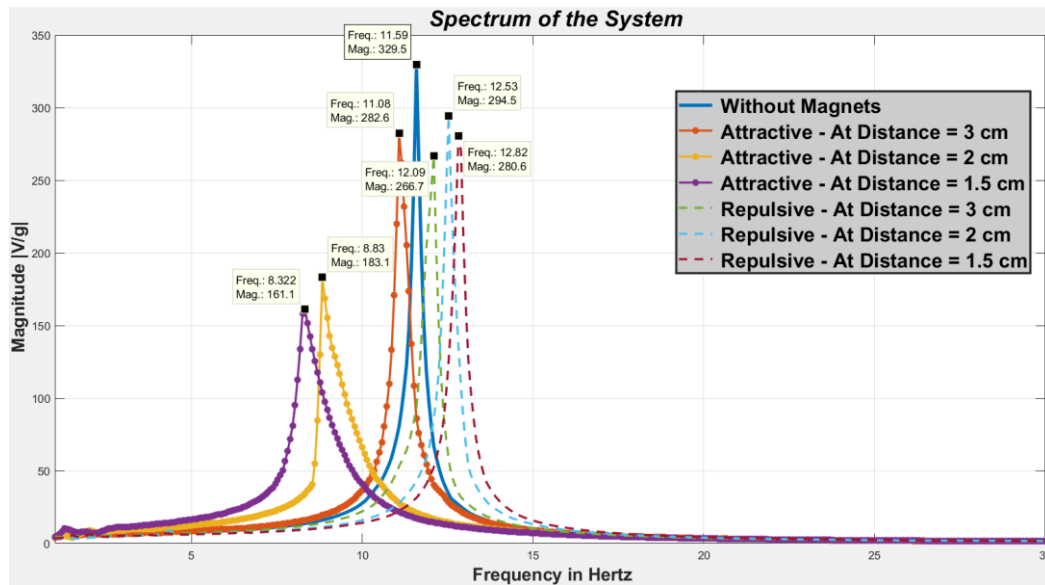


Fig. 7 - The experimental results for the output voltage for PEH with one of the side fixed magnets

Through observations, the frequency bandwidth increases in attractive mode, as it reaches to 0.425 Hz and 0.62 Hz at 2 cm and 1.5 cm respectively. However, the peak output voltage decreases whilst the distance decreases at attractive mode, as it reaches to 161.1 V/g at 1.5 cm. This is due to the inverse relationship between bandwidth and output voltage. In general, the pattern given by both simulation and the experimental results yield the same observation. The resonance frequency of the beam increases in the case of the repulsive mode, while decreasing the distance, and decreases in the attractive mode. The peak power achieved in the repulsive mode has a gradual decrement while decreasing the distance. Also, the bandwidth achieved in the attractive mode is the largest amongst other plots. The measurements of the output voltage, frequency bandwidth, and the resonance frequency are summarized in Table 3.

Table 3 - Summary of the experimental results for PEH with one fixed magnet for different cases

Polarity	D _o (cm)	Peak Voltage, V _p	Frequency bandwidth (Hz)	Natural Frequency, ω _n (Hz)
		$\left \frac{V}{g} \right $		
No Magnets	-	329.5	0.20	11.59
Attractive	3.0	282.6	0.35	11.08
Attractive	2.0	183.1	0.43	8.83
Attractive	1.5	161.1	0.62	8.32
Repulsive	3.0	266.7	0.34	12.09
Repulsive	2.0	294.5	0.26	12.53
Repulsive	1.5	280.6	0.30	12.82

4. Conclusion

This paper reports simulation and experimental studies of piezoelectric energy harvester (PEH) with magnetic field. The simulation was successfully done using COMSOL Multiphysics software to include the effect of magnetic field on the performance of piezoelectric energy harvester. In the simulation, only attractive mode is considered, and it shows that using magnetic oscillator shows a more promising result as compared to the PEH with fixed magnet and conventional PEH, with an increase of 10% frequency bandwidth. On the other hand, in the experiment, a thorough analysis can be made experimentally involving variations of distances and polarities. It is seen that, in attractive mode, larger bandwidth is observed, and the natural frequency is seen to be shifted to the right, as compared to the repulsive mode. The largest frequency bandwidth is found at attractive mode, with an increment of 210%, at a distance of 1.5 cm. In general, the presence of magnet in a piezoelectric energy harvesting system, using either permanent magnet or magnetic oscillator, do provide enhancement in terms of frequency bandwidth.

Acknowledgement

This work was supported by IIUM Research Acculturation Grant Scheme (IRAGS18-020-0021). The author would like to thank Department of Mechatronics of International Islamic University Malaysia for the opportunity to conduct the research.

References

- [1] Chai, Zhisheng et al. (2016). "Tailorable and Wearable Textile Devices for Solar Energy Harvesting and Simultaneous Storage." *ACS Nano* 10(10)
- [2] Yang, Zhengbao, and Jean Zu. (2016). "Comparison of PZN-PT, PMN-PT Single Crystals and PZT Ceramic for Vibration Energy Harvesting." *Energy Conversion and Management* 122
- [3] Fu, Hailing, Zahra Sharif-Khodaei, and Ferri Aliabadi. (2019). "A Bio-Inspired Host-Parasite Structure for Broadband Vibration Energy Harvesting from Low-Frequency Random Sources." *Applied Physics Letters* 114(14)
- [4] Muthalif, Asan G.A., and N. H.Diyana Nordin. (2015). "Optimal Piezoelectric Beam Shape for Single and Broadband Vibration Energy Harvesting: Modeling, Simulation and Experimental Results." *Mechanical Systems and Signal Processing* 54
- [5] Saadatnia, Zia et al. (2017). "Modeling and Performance Analysis of Duck-Shaped Triboelectric and Electromagnetic Generators for Water Wave Energy Harvesting." *International Journal of Energy Research* 41(14)
- [6] Hao, Congcong et al. (2019). "Two-Dimensional Triboelectric-Electromagnetic Hybrid Nanogenerator for Wave Energy Harvesting." *Nano Energy* 58
- [7] Wei, Chongfeng, and Xingjian Jing. (2017). "A Comprehensive Review on Vibration Energy Harvesting: Modelling and Realization." *Renewable and Sustainable Energy Reviews* 74
- [8] Covaci, Corina, and Aurel Gontean. (2020). "Piezoelectric Energy Harvesting Solutions: A Review." *Sensors (Switzerland)* 20(12)
- [9] Jiang, Shu Nong, Shao Hua Guo, and Xian Fang Li. (2012). "Performance Analysis for a Unimorph Cantilever Piezoelectric Harvester." *Zhendong yu Chongji/Journal of Vibration and Shock* 31(19)
- [10] Fakhzan, M. N., and Asan G.A. Muthalif. (2013). "Harvesting Vibration Energy Using Piezoelectric Material: Modeling, Simulation and Experimental Verifications." *Mechatronics* 23(1)
- [11] Moon, Kyuchang et al. (2018). "A Method of Broadening the Bandwidth by Tuning the Proof Mass in a Piezoelectric Energy Harvesting Cantilever." *Sensors and Actuators, A: Physical* 276
- [12] Lou, Liang et al. (2016). "Comparative Characterization of Bimorph and Unimorph AlN Piezoelectric Micro-Machined Ultrasonic Transducers." In *Proceedings of the IEEE International Conference on Micro Electro Mechanical Systems (MEMS)*,
- [13] Batra, Ashok et al. (2020). "Design of a Unique Unimorph and Bimorph Cantilever Energy Harvesting System." *Advanced Science, Engineering and Medicine* 12(4)
- [14] Krishnasamy, M. et al. (2020). "Design and Simulation of Smart Flooring Tiles Using Two-Phased Triangular Bimorph Piezoelectric Energy Harvester." In *Proceedings of 2020 IEEE-HYDCON International Conference on Engineering in the 4th Industrial Revolution, HYDCON 2020*,
- [15] Hosseini, Rouhollah, and Mohsen Hamedi. (2016). "Resonant Frequency of Bimorph Triangular V-Shaped Piezoelectric Cantilever Energy Harvester." *Journal of Computational and Applied Research in Mechanical Engineering* 6(1)
- [16] Kumar, Anuruddh et al. (2018). "A Comparative Numerical Study on Piezoelectric Energy Harvester for Self-Powered Pacemaker Application." *Global Challenges* 2(1)
- [17] Murthy, K. S.M. et al. (2017). "Fem Simulation of Ultra Low Resonant Piezoelectric Spiral Energy Harvester." *Journal of Advanced Research in Dynamical and Control Systems* 9(Special issue 14)
- [18] Li, Haisheng et al. (2020). "Broadband Bimorph Piezoelectric Energy Harvesting by Exploiting Bending-Torsion of L-Shaped Structure." *Energy Conversion and Management* 206
- [19] Kim, Jaegyung et al. (2020). "Cost-Effective and Strongly Integrated Fabric-Based Wearable Piezoelectric Energy Harvester." *Nano Energy* 75
- [20] He, Xianming et al. (2021). "Theoretical and Experimental Studies on MemS Variable Cross-Section Cantilever Beam Based Piezoelectric Vibration Energy Harvester." *Micromachines* 12(7)
- [21] Palosaari, Jaakko et al. (2012). "Energy Harvesting with a Cymbal Type Piezoelectric Transducer from Low Frequency Compression." *Journal of Electroceramics* 28(4)
- [22] Shi, Qiongfeng, Tao Wang, and Chengkuo Lee. (2016). "MEMS Based Broadband Piezoelectric Ultrasonic Energy Harvester (PUEH) for Enabling Self-Powered Implantable Biomedical Devices." *Scientific Reports* 6
- [23] Jeong, Se Yeong et al. (2016). "Design of a Multi-Array Piezoelectric Energy Harvester for a Wireless Switch." *International Journal of Hydrogen Energy* 41(29)
- [24] Tang, Lihua, and Yaowen Yang. (2012). "A Nonlinear Piezoelectric Energy Harvester with Magnetic Oscillator." *Applied Physics Letters* 101(9)